Hindawi
Journal of Spectroscopy
Volume 2022, Article ID 5502651, 9 pages
https://doi.org/10.1155/2022/5502651

Research Article

Multiscale-Band *K*-Distribution Model for Molecules in High-Temperature Gases

Lei Shi,[1,2] **Yuyue Zhang**,[1,2] **Fangyan Li**,[1,2] **Yuefan Du**,[1,2] **and Bo Yao**[1,2]

[1]*School of Aerospace Science and Technology, Xidian University, Xi'an City, China*
[2]*Key Laboratory of Equipment Efficiency in Extreme Environment, Ministry of Education, Xidian University, Xi'an City, China*

Correspondence should be addressed to Fangyan Li; lfybhang@163.com

Received 9 February 2022; Accepted 23 May 2022; Published 15 June 2022

Academic Editor: Jau-Wern Chiou

Radiation heat transfer plays a dominant role in high-temperature flow field. Rapid and reliable calculation of spectral radiation properties is beneficial for thermal analysis and detection of radiation target. In this paper, a multiscale-band *k*-distribution model is proposed for the study of radiation properties in high-temperature gases. The accurate absorption coefficients are firstly calculated using the line-by-line model. The slope of the accurate absorption coefficient line and its slope threshold are then extracted and analyzed, which act as a basis to divide the absorption coefficient line into multiple segments. For different segments, different bandwidths are chosen for the corresponding band *k*-distribution model. In the model, the 7-point Gauss–Lobatto method is employed to obtain the optimized absorption coefficients. These optimized absorption coefficients formed the absorption coefficient database. The radiation intensities of gases are finally calculated and analyzed based on the optimized database. Experimental results suggest that the multiscale-band *k*-distribution model can improve the efficiency up to 35% compared with the widely used narrow-band *k*-distribution model. Simultaneously, the relative calculation error is less than 5% compared with the most accurate line-by-line model.

1. Introduction

Gas radiation properties are commonly used in various research fields, including atmospheric radiation transferring, atmospheric remote sensing, and ecological monitoring [1–3]. They also exhibit outstanding advantages in space-based applications, such as spectral detection, thermal protection, and hypersonic target detection and tracking [4–6]. In the detection and identification of hypersonic aircraft, the detailed information of altitude, velocity, and type of aircraft can be obtained effectively by analyzing the radiation properties of plasma sheath around the reentry stage of aircraft, which is of great significance in military confrontation.

In recent years, the development of space technology has driven advances in the calculation of radiation properties. A variety of calculation models have been established for the calculation of the radiation properties, which can be categorized into the global model [7], surrogate model [8], line-by-line (LBL) model [9], and band model. Among these models, the LBL model is the most accurate one but is time-consuming because it considers the superposition of each spectral line. The global model is generally used for analyzing the whole spectrum radiation in practical engineering. The surrogate model has relative high computational efficiency, but the calculated results are often difficult to analyze. The band model can characterize the spectra structure in detail while significantly reducing the required computational time. The superior capability of the band model enables its wide use in academic research and engineering applications. Band models can be classified into narrow band and wide band ones according to the spectral resolution. The Elsasser model is recognized as the simplest narrow band mode for calculating the parameters of diatomic and polyatomic molecules. In 1990s, the statistical narrow band correlated-k model (SNBCK) was proposed to solve the problem of scattering in the field of thermal radiation transfer [10]. The commonly used wide band models for practical scenarios are

the box model (BM) [11], the Edwards model (EWB) [12], and the wide band k-distribution model (WBK) [13]. Recent advances in band models are mainly based on the k-distribution function. For example, Bansal et al. [14] presented a k-distribution model for gas mixtures in thermodynamic nonequilibrium, where the radiative transfer equations are solved separately for each emitting species and overlap with other species is treated in an approximate way. Hu et al. [15] deduced an improved spectral absorption coefficient grouping strategy of wide band k-distribution model used for calculating the infrared remote sensing signal of hot exhaust systems. Kez [16] conducted a comprehensive evaluation on the results of different models, including the statistical narrow band (SNB) model, the SNBCK model, the WBCK model, the FSCK model, and the WSGG model.

The aforementioned narrow band and wide band models exhibit both advantages and disadvantages in terms of algorithm complexity, efficiency, and accuracy. Generally, the narrow band model is more accurate than the wide band model and is more suitable for the study of the spectral radiation properties. The wide band model neglects the details of spectral line characteristics, and the data of the whole vibration-rotation band are processed directly. Therefore, the wide band model has high computational efficiency with large error and is mostly used in engineering applications. For space-based applications, the space target is characterized with high speed, far distance, and complex background, which would result in complex spectral characteristics over the whole spectrum range. The current wide band models cannot satisfy practical requirements of complex spectral characteristics. To better characterize the spectral radiations of the space target, there is an urgent need for introducing more accurate and effective solution models. In particular, for models that possess superior performance to existing methods, complex and time-consuming procedures are not required.

To resolve the above issues, in this paper, we propose a multiscale-band k-distribution (MSBK) model to optimize the calculation of radiation properties. The proposed model partitions the spectral wave-band into several segments according to the line trend of the accurate absorption coefficients obtained by the LBL model. The absorption coefficients at different segments are processed by the band k-distribution model with different bandwidths to improve the computational efficiency while ensuring the accuracy. The remainder of this paper is organized as follows: Section 2 introduces the computational method. Section 3 conducts the model validation. Section 4 outlines the corresponding results and discussion. Section 5 summarizes conclusions of this paper.

2. Computational Method

The accurate determination of radiation properties depends on three aspects, i.e., accurate spectral data, efficient model for spectral radiation, and the reliable the radiative transfer equation (RTE) solution model. In this section, the method for calculating radiation properties is explained first. Then, the MSBK model is proposed to optimize the calculation of radiation properties. The spectral data are obtained based on HITEMP [17] and HITRAN [18] databases. The MSBK model is adopted for spectral radiation. The radiation intensity is obtained by solving RTE.

2.1. Calculation of Radiation Properties. The parameters of the gas radiation property model are generally described by absorption coefficients. These parameters can be obtained either from the experiment or from the spectroscopic database-based calculation. In practical applications, the molecular line-broadening effect occurs near the center frequency of the absorption line. Therefore, the absorption coefficient k_σ [19] of a molecule at wave number σ is the sum of all absorption lines at σ, which can be expressed as

$$k_\sigma = \sum_i S_i(\sigma_{0i}) F(\sigma - \sigma_{0i}), \tag{1}$$

where S_i is the intensity of the ith line at the center wave number σ_{0i} and the term $F(\sigma\text{-}\sigma_{0i})$ is the normalized function of line broadening.

The absorption coefficient of the mixed gases can be obtained by the correlation or noncorrelation methods [20]. The noncorrelation method is employed here due to its small error and high efficiency. In the noncorrelation method, it is assumed that the statistical independence exists among the absorption coefficients of different gases, which can be regarded as random variables. The absorption coefficient k_σ of a mixture of several gases can therefore be obtained by the sum of the absorption coefficient $k_{i,\sigma}$ of each species i, which can be expressed as

$$k_\sigma = \sum_i k_{i,\sigma}. \tag{2}$$

The transmittance τ_σ at wave number σ with distance L is [21] written as

$$\tau_\sigma = \exp[-k_\sigma \cdot L]. \tag{3}$$

The radiative transfer equation (RTE) that neglects the scattering can be expressed as [22]

$$\frac{\mathrm{d}I_\sigma(s)}{\mathrm{d}s} = -k_\sigma I_\sigma(s) + k_\sigma I_{b\sigma}(s), \tag{4}$$

where k_σ is the absorption coefficient and I_σ and $I_{b\sigma}$ are the local spectral intensity and Planck blackbody radiation intensity at the s location, respectively.

The RTE can be solved by using the line of sight (LOS) method. Specifically, during the calculation of LOS, an LOS line is divided into N segments corresponding to the layers of the flow field. Each layered medium is assumed to be uniform, isotropic, and isothermal. A single LOS line has a known and continuous transmission path inside the flow field, along which the radiation intensity is determined by the distribution of temperature, pressure, and gas concentration. The intensity of absorption and emission in each layer is calculated layer by layer along the LOS line. The radiation intensity along the LOS line can be written as

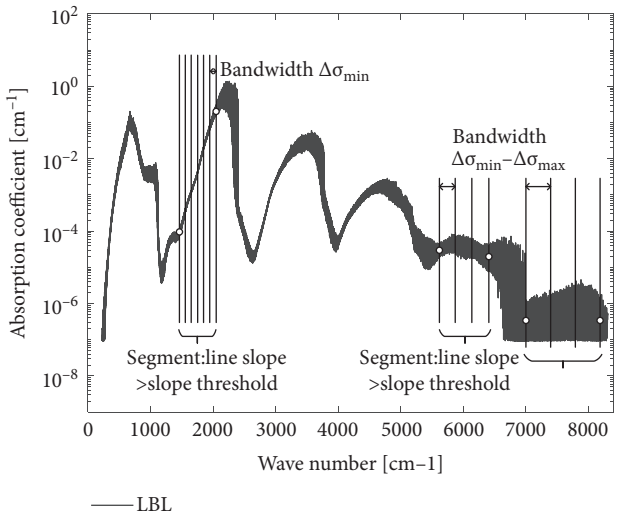

Figure 1: Schematic diagram of waveband division in the MSBK model.

$$I_\sigma^n = \left[1 - \tau_\sigma^n\right] I_\sigma^{n-1} + \tau_\sigma^n I_{b\sigma}^n, \tag{5}$$

where n denotes the layer number, I_σ^n is the radiation intensity at the n-th layer, and the multiplication of the spectral absorption coefficient and the path length, $\tau_\sigma{}^n = \exp(-k_\sigma{}^n L)$, is defined as the optical thickness.

When solving equation (5), the integral scheme of the band k-distribution models adopted in this research is the key factor to obtain the radiation intensity efficiently and accurately. An efficient method needs to be introduced to ensure accuracy and efficiency. Therefore, a widely used 7-point Gauss–Lobatto quadrature [23] method is employed here, which has the highest calculation accuracy. The main purpose of this method is to simplify calculations by replacing integral with accumulation. Seven integral points and weight factors are provided in this method, and only seven calculations are required to solve the RTE. Equation (5) can be solved by obtaining seven values for the radiation intensity in a waveband:

$$I_{\sigma i,m}^n = \left[1 - \tau_{\sigma i,m}^n\right] I_{\sigma i,m}^{n-1} + \tau_{\sigma i,m}^n I_{b\sigma}^n, \tag{6}$$

where the subscripts m and σi denote the absorption coefficient point and the number of the wavebands, respectively.

The average intensity of the σi-th band is written as

$$I_{\sigma i} = \sum_{j=1}^{7} \omega_j I_{g_j,\sigma i}, \tag{7}$$

where g_j and ω_j are the integral points and weight factors of the quadrature, respectively.

2.2. Multiscale-Band K-Distribution Model. In the narrow band, the Planck function can be approximated as a constant, so the radiation intensity in the band is only a function of the absorption coefficient. The traditional k-distribution method reorders the absorption coefficient into a smooth and monotone increasing function, during which each absorption coefficient value is calculated only once.

According to the k-distribution method [19], the probability density function (PDF) of the absorption coefficient can be written as

$$f(k) = \frac{1}{\Delta\sigma} \int_{\Delta\sigma} \delta(k - k_\sigma) d\sigma = \frac{1}{\Delta\sigma} \sum_i \left| \frac{d\sigma}{dk_\sigma} \right|_i, \tag{8}$$

where $\Delta\sigma$ is the wave number interval and δ(k) is the Dirac delta function.

The cumulative distribution function is given by

$$g(k) = \int_0^k f(k') dk'. \tag{9}$$

In equation (9), $g(k)$ is a monotone increasing function ranging from $g(k_{\min}) = 0$ to $g(k_{\max}) = 1$, with $k_{\min}$ and $k_{\max}$ being the minimum and maximum values of k_σ inside $\Delta\sigma$.

According to equations (8) and (9), the same bandwidth was employed over the whole spectrum for the traditional NBK model. In this case, although the computational accuracy can be guaranteed, the computational efficiency cannot be taken into account simultaneously. Therefore, a multiscale-band k-distribution (MSBK) model on the basis of the narrow band k-distribution (NBK) model was proposed. The principle of the proposed model is shown in Figure 1. Firstly, the accurate absorption coefficient line obtained by the LBL model was divided into multiple segments according to the slope of the line and the given slope threshold. For different segments, different bandwidths were then chosen for the corresponding k-distribution model. The minimum bandwidth was adopted in the segments where the slope of the absorption coefficient line was greater than the given slope threshold, and different bandwidths within range $\Delta\sigma_{min}$–$\Delta\sigma_{max}$ were adopted in other segments. It was a tradeoff of the calculation accuracy and efficiency.

During the MSBK model, the accurate absorption coefficient line was firstly obtained by the LBL model. Then, the corresponding slope of each point on the accurate absorption coefficient line was calculated. The accurate absorption coefficient line was divided into multiple narrow bands with bandwidth $\Delta\sigma$, and the average absorption coefficient in each narrow band was obtained. The slope of the spectral line in the i-th band can be obtained by

$$k\prime(\sigma_{i-1}) = \frac{\left[-3\overline{k}(\sigma_{i-1}) + 4\overline{k}(\sigma_i) - \overline{k}(\sigma_{i+1})\right]}{2\Delta\sigma}, \tag{10}$$

$$k\prime(\sigma_i) = \frac{\left[-\overline{k}(\sigma_{i-1}) + \overline{k}(\sigma_{i+1})\right]}{2\Delta\sigma}, \tag{11}$$

$$k\prime(\sigma_{i+1}) = \frac{\left[\overline{k}(\sigma_{i-1}) - 4\overline{k}(\sigma_i) + \overline{k}(\sigma_{i+1})\right]}{2\Delta\sigma}, \tag{12}$$

where $\overline{\ }$k(σi) is the average absorption coefficient in the i-th narrow band whose central wave number is σi and $k'(\sigma i)$ is the slope of the spectral line in the i-th narrow band.

The slope threshold is the key factor to ensure the efficiency and precision of the MSBK model. In order to obtain

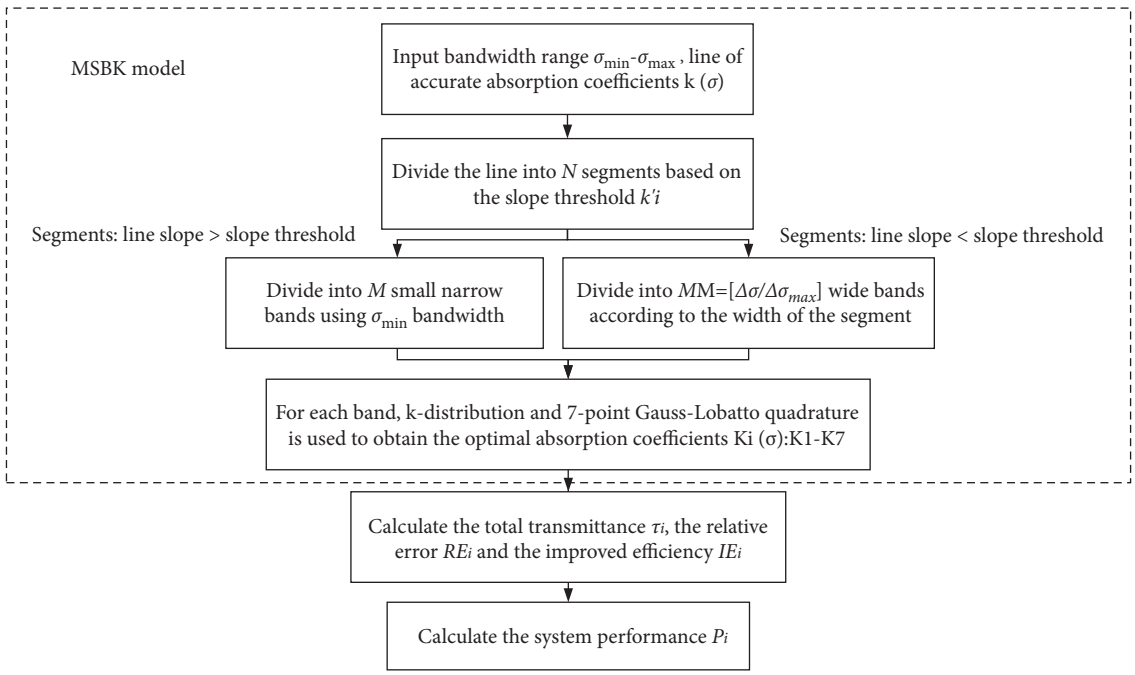

Figure 2: Flow chart of system performance calculation.

the optimal slope threshold, several appropriate samples of the slope threshold were selected, and the system performance P for each sample point was calculated. For the i-th sample point k'_i, the calculation process of system performance P_i is shown in Figure 2.

The system performance P is evaluated by the relative error and improved efficiency. A high system performance represents high improved efficiency and low relative error. Here, the relative error and improved efficiency were calculated by the total transmittance obtained from different models. The total transmittance τ [24] can be expressed as

$$\tau_\sigma = \frac{I_\sigma(L)}{I_\sigma(0)} = \exp(-k_\sigma L), \tag{13}$$

$$\tau = \frac{\int_0^\infty \tau_\sigma I_\sigma(0)\mathrm{d}\sigma}{\int_0^\infty I_\sigma(0)\mathrm{d}\sigma}, \tag{14}$$

where $\tau\sigma$ is the transmittance at wave number σ and the function Iσ(L) is the radiation intensity at distance L.

Then, the relative error (RE) and the improved efficiency (IE) can be expressed as

$$RE = \frac{|\tau_{MNBK} - \tau_{LBL}|}{\tau_{LBL} < RE_{\text{line}}}, \tag{15}$$

$$IE = \frac{(t_{LBL} - t_{MNBK})}{t_{LBL} > IE_{\text{line}}}, \tag{16}$$

where REline and IEline are the maximum permissible relative error and the minimum improved efficiency, respectively. Here, REline is set as 5% and IEline as 95%, and the sample points that do not satisfy the required conditions are negligible.

Based on the above results, the system performance P_i of the i-th sample point can be obtained by

$$P_i = 0.5 \cdot \frac{IE_i - IE_{\min}}{IE_{\max} - IE_{\min}} + 0.5 \cdot \frac{RE_{\max} - RE_i}{RE_{\max} - RE_{\min}}, \tag{17}$$

where REmin and REmax are the maximum and minimum permissible relative error, respectively. IEmin and IEmax are the maximum and the minimum improved efficiency, respectively. In addition, larger P suggests better system performance.

The aforementioned calculation process with different sample points k'i is repeated, and then the system performance Pi of all sample points was calculated. Finally, the optimum slope threshold was obtained, which was the sample point of the maximum system performance. Based on the optimal slope threshold, the optimized gas absorption coefficients were obtained by the MSBK model as shown in Figure 2.

The wavebands where the line slope is lower than the slope threshold are wider. Therefore, the Planck function can no longer be regarded as a constant in calculating the blackbody radiation. The Planck function can be corrected by a correction factor as

$$\varphi = \frac{\overline{I}_{b\sigma}}{I_{b\sigma}} = \frac{\int_\sigma^{\sigma+\Delta\sigma}\left(I_{b\sigma\prime}/\sigma\prime\right)\mathrm{d}\sigma\prime}{I_{b\sigma}} = \frac{\sum_{i=1}^n I_{b\sigma i}\Delta\sigma_i}{I_{b\sigma}\Delta\sigma}. \tag{18}$$

3. Model Validation

The division of spectral wave-band based on the slope threshold is of great significance for the accuracy and efficiency of the MSBK model. Therefore, the influence of the

band-width on the total transmittance of the NBK model is analyzed in this section to determine the appropriate bandwidth range. Then, the selected bandwidth is substituted into to the MSBK model to calculate the total transmittance. Since the absorption coefficient is associated with the gas species, temperature, and pressure, only the effects of temperature, pressure, and gas mole fraction on the optimum slope threshold are finally analyzed. Since CO_2 is one of the most active gas species in radiation properties, it is taken as an example for model verification.

The effect of bandwidths on total transmittance at different distances is given in Figure 3. As illustrated, the NBK model with 200 cm^{-1} bandwidth has the largest relative error, while the model with 25 cm^{-1} to 100 cm^{-1} bandwidths has almost the same errors. In general, the total transmittance obtained by the LBL model and the NBK model with different bandwidths exhibited almost no discrepancy. However, as smaller bandwidth of the NBK model was employed, more computation is required. Therefore, considering the calculation accuracy and efficiency comprehensively, the bandwidth ranging from 25–100 cm^{-1} is therefore adopted in the following verification.

Figure 4 shows the correlation between the optimum slope threshold and the temperature, the pressure, and the mole fraction under uniform isothermal medium at a distance of 10 m. The fitting results suggest that the optimum slope threshold increases linearly with temperature. The effects imposed by the pressure and the mole fraction on the optimum slope threshold are negligible. Therefore, only the influence of temperature is needed for calculating the optimal slope threshold of different species. The optimal slope threshold of CO_2 at different temperatures can be obtained from Figure 4.

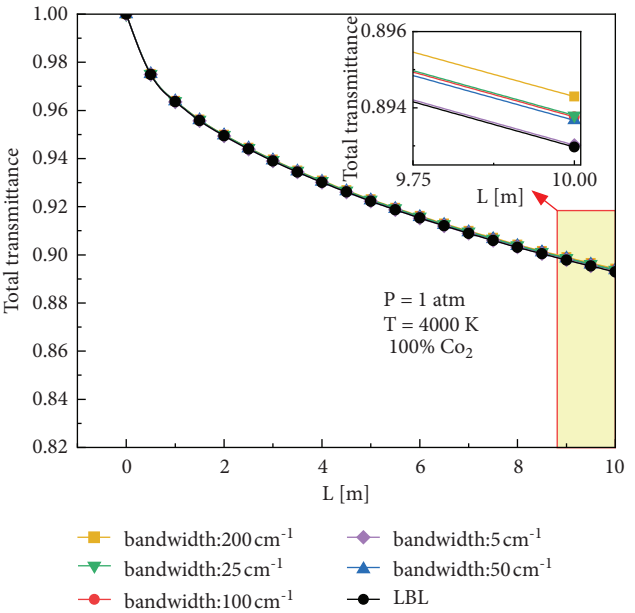

Figure 3: Effect of bandwidth on the total transmittance.

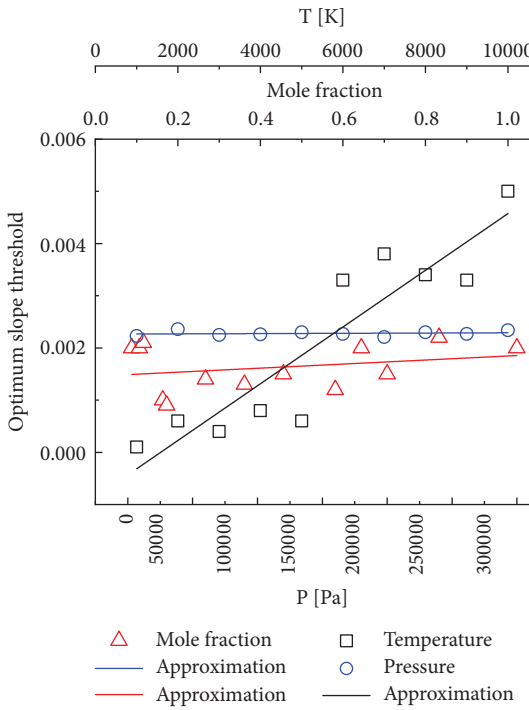

Figure 4: Correlation between the optimum slope threshold and the temperature, pressure, and mole fraction.

4. Results and Discussion

The CO_2, CO, and H_2O are active gas species of radiation properties in most engineering applications. In this section, the proposed MSBK model was used to calculate the radiation intensities of CO_2, CO, and H_2O mixture gases in isothermal medium and the pure CO_2 gas in the nonisothermal medium. The calculated results were compared with the experimental data [20, 25]. The accuracy and efficiency of the MSBK model were analyzed and compared with those of the NBK model.

For nonisothermal medium, the RTE can be solved with the LOS approach. Figure 5 shows the radiation intensity of CO_2 at 2.7 μm obtained from HITRAN and HITEMP databases, to which the high-temperature conditions are listed out in Table 1. The EXP line is obtained from the experiment [20]. It can be observed from the figure that the results calculated by MSBK model based on different databases are all in good consistency with the experimental data, with all the relative errors below 5%.

For the mixed gases, Figure 6 shows the comparison of experimental data and spectral intensities calculated by the LBL model and the MSBK model. The flow field data adopted in the calculation are obtained from the experiment [25]. It can be observed from Figure 6 that, for the calculation of radiation intensities in the mixed gases, the results match well with the experimental data. The total relative error is less than 5%. The results are slightly lower than the experimental data at the waveband of 3.5–4.0 μm, which may

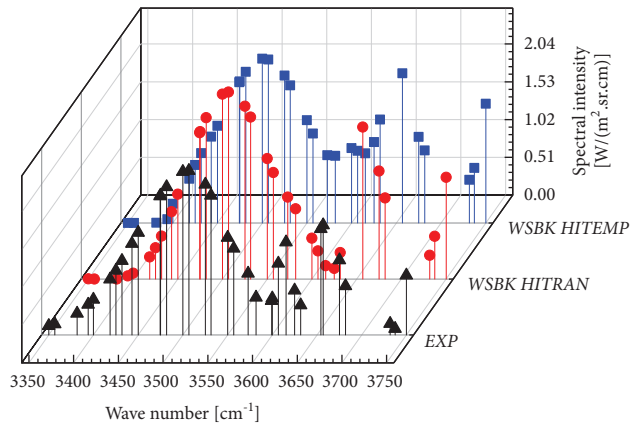

Figure 5: Spectral intensity of CO_2 at 2.7 μm.

Table 1: Layer and temperature ($P = 1$ atm; $L = 6$ cm).

Layer	1	2	3	4	5	6	7	8	9	10
T (K)	386	528	719	953	1130	1160	979	737	541	387

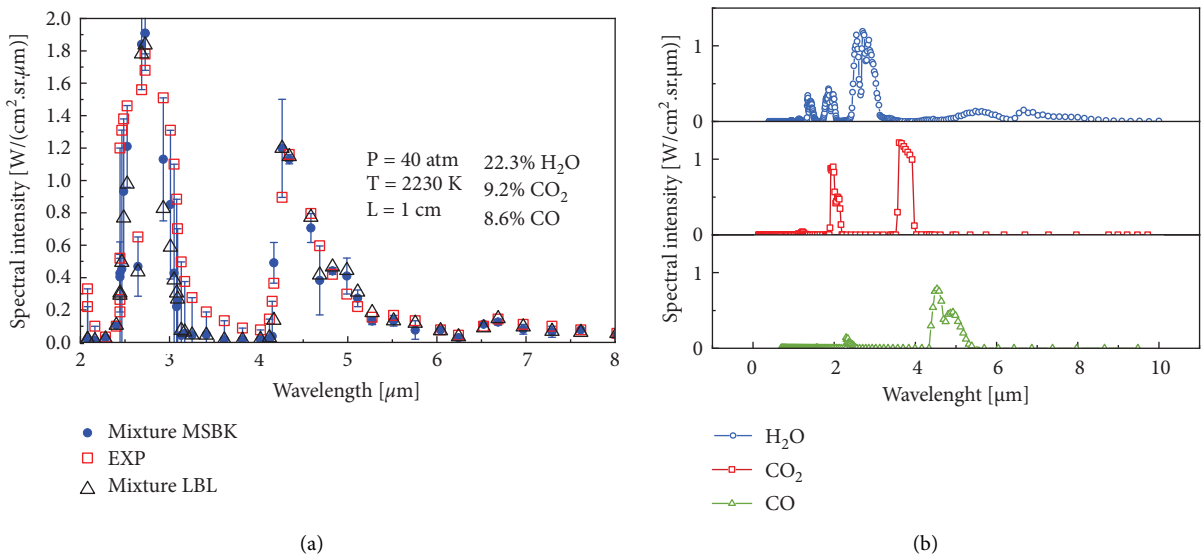

Figure 6: Comparison of experimental data and calculated spectral intensities using the MSBK model.

attribute to the neglected scattering during the calculation. As can be seen from the above results, the proposed MSBK model can well calculate the radiation properties of the high-temperature gases.

The accuracy and efficiency of the MSBK model are analyzed as follows. Taking nonisothermal CO_2 medium as an example, the total radiation intensities under different transmission distances were calculated based on the MSBK, NBK, and LBL models, respectively. The environmental conditions are shown in Table 1. Compared with the LBL model, the relative errors of the MSBK model and NBK model were analyzed. Compared with the NBK model, the improved efficiencies of the MSBK model were calculated. Figure 7 shows the accuracy and efficiency of the MSBK model for the total radiation intensity of CO_2 at 0–10000 cm^{-1}. Figure 7(a) shows the relative errors of total radiation intensities obtained by the MSBK model and by the NBK model compared with the LBL model. Figure 7(b) shows the improved efficiency of the MSBK model compared with the NBK model. The results suggest that, as the transmission distance increases, the improved efficiency is about 16%, the average relative error is less than 5%.

In order to further analyze the accuracy and efficiency of the MSBK model, HITEMP with larger data volume was used to calculate the radiation intensity. The effects of different bandwidth ranges on the accuracy and efficiency of the MSBK model were also analyzed. Figure 8 shows the accuracy and efficiency of the MSBK model at different

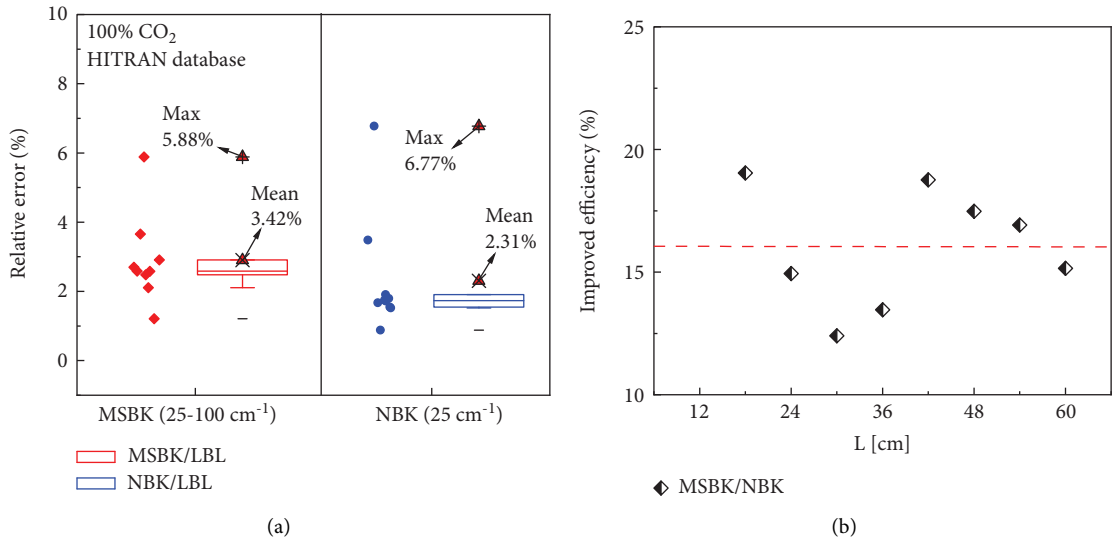

Figure 7: Accuracy and efficiency of MSBK model in a nonisothermal medium.

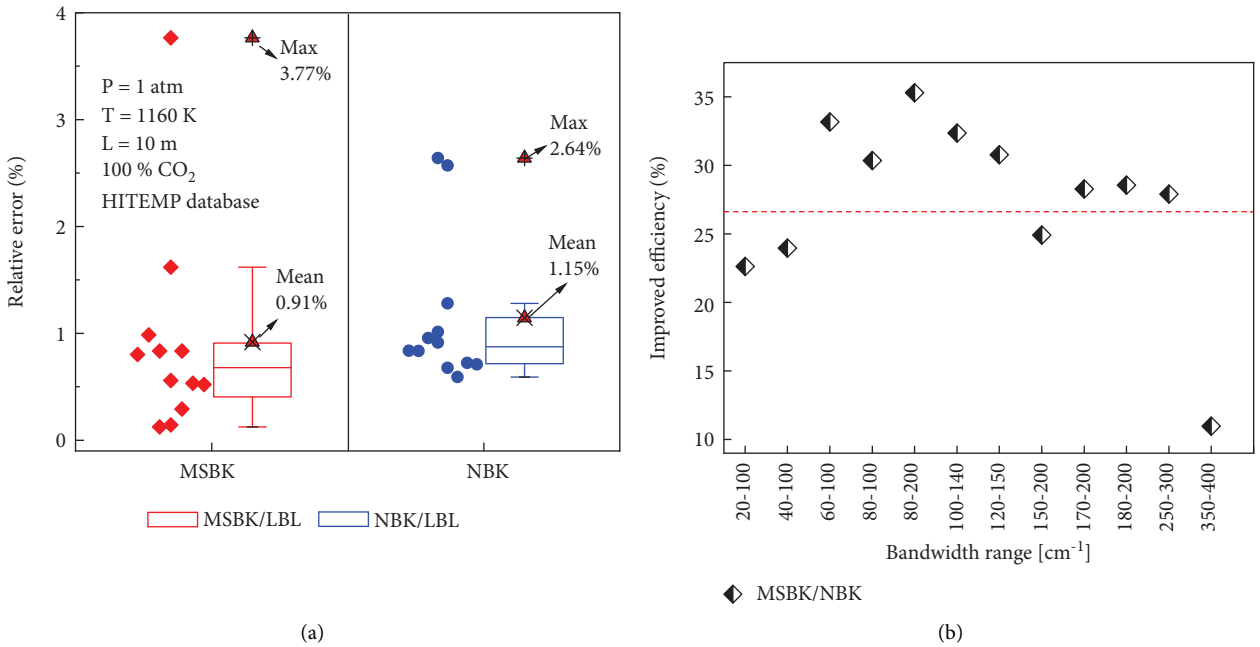

Figure 8: Accuracy and efficiency of the MSBK model at different bandwidth ranges.

bandwidth ranges. It can be observed that, as the bandwidth range increases, the average improved efficiency is 27%, and the maximum is 35%. When the bandwidth range increases to 400 cm^{-1}, the relative error increases, and the improved efficiency decreases.

In summary, the proposed MSBK model can be employed to obtain the radiation intensity efficiently and accurately:

(1) For the nonisothermal medium, the relative error of the MSBK model is slightly higher than that of the NBK model, but the efficiency is significantly improved.

(2) For an appropriate bandwidth, the relative errors of the proposed MSBK model are less than 5% compared with the LBL model, which is similar to the NBK model. But compared with the NBK model, the improved efficiency is up to 35%.

(3) Extension of the bandwidth range and increase of the number of absorption lines can also improve the calculation efficiency to a certain extent.

5. Conclusions

Considering the practical application requirements of the radiation properties, a MSBK model was proposed for the efficient and accurate calculation of radiation properties in the high-temperature gases, particularly H_2O and CO_2. The

proposed model divides the spectral waveband into several segments, according to the line trend of the accurate absorption coefficients obtained by the LBL model. The spectrum band can be processed flexibly by using a small or a large bandwidth, thereby ensuring the accuracy while maximizing the efficiency. Simulation results show that the relative errors of the proposed model are less than 5% compared with the LBL model, with the improved efficiency of being up to 35% compared with the NBK model. Furthermore, the moderate extension of the bandwidth range and increase of the absorption lines can improve the computing efficiency.

The proposed MSBK model is compatible for various methods of RTE solution and is suitable for calculating radiation properties in particular at the entire spectrum ranges. The radiation intensity obtained by this model can provide reference data for hypersonic target detection and tracking.

Data Availability

No data were used to support this study.

Conflicts of Interest

The authors declare that they have no conflicts of interest.

Acknowledgments

This study was supported by the National Natural Science Foundation of China (Grant nos. 61871302, 62101406, and 62001340) and the Fundamental Research Funds for the Central Universities (Grant no. JB211311).

References

[1] K. Sassen and J. M. Comstock, "A Midlatitude Cirrus Cloud Climatology from the Facility for Atmospheric Remote Sensing. Part III: Radiative Properties," *Journal of the Atmospheric Sciences*, vol. 58, no. 15, p. 2113, 2001.

[2] J. Yue, J. Tian, N. Xu, and Q. Tian, "Vegetation-shadow indices based on differences in effect of atmospheric-path radiation between optical bands," *International Journal of Applied Earth Observation and Geoinformation*, vol. 104, Article ID 102579, 2021.

[3] E. Marenkov, S. Krasheninnikov, and A. Pshenov, "Multilevel model of radiation transport in inhomogeneous plasma," *Contributions to Plasma Physics*, vol. 58, no. 6-8, pp. 570–577, 2018.

[4] M. Ferraiuolo and O. Manca, "Heat transfer in a multi-layered thermal protection system under aerodynamic heating," *International Journal of Thermal Sciences*, vol. 53, pp. 56–70, 2012.

[5] Y. S. Zhao and X. P. Du, "Modeling of the radiation properties of flow around the hypersonic aircrafts," *Applied Mechanics and Materials*, vol. 556-562, pp. 1338–1341, 2014.

[6] R. Liang, Y. Liu, and F. Li, "Partition functions of atomic and diatomic species in high-temperature atmospheric plasmas," *Contributions to Plasma Physics*, vol. 61, no. 8, Article ID e202100036, 2021.

[7] L. Pierrot, P. Rivière, A. Soufiani, and J. Taine, "A fictitious-gas-based absorption distribution function global model for radiative transfer in hot gases," *Journal of Quantitative Spectroscopy and Radiative Transfer*, vol. 62, no. 5, pp. 609–624, 1999.

[8] T. Ren, M. F. Modest, A. Fateev, G. Sutton, W. Zhao, and F. Rusu, "Machine learning applied to retrieval of temperature and concentration distributions from infrared emission measurements," *Applied Energy*, vol. 252, Article ID 113448, 2019.

[9] L. Sparks, "Efficient line-by-line calculation of absorption coefficients to high numerical accuracy," *Journal of Quantitative Spectroscopy and Radiative Transfer*, vol. 57, no. 5, p. 631, 1997.

[10] F. Liu, G. J. Smallwood, and O. L. Gulder, "Application of the statistical narrow-band correlated-k method to non-grey gas radiation in CO2–H2O mixtures: approximate treatments of overlapping bands," *Journal of Quantitative Spectroscopy and Radiative Transfer*, vol. 68, no. 4, p. 401, 2001.

[11] Y. Liu and X. Zhang, "Analysis of gas radiative transfer using box model and its comparison with gray band approximation," *Journal of Thermal Science*, vol. 12, no. 1, pp. 82–88, 2003.

[12] D. K. Edwards, "Molecular Gas Band Radiation," *Advances in Heat Transfer*, vol. 12, p. 115, 1976.

[13] X. M. Yin, L. H. Liu, and B. X. Li, "Numerical simulation of infrared signature emitted by liquid rocket plume using wide band K-distribution model," *Advanced Materials Research*, vol. 516-517, pp. 41–53, 2012.

[14] A. Bansal, M. F. Modest, and D. A. Levin, "Multi-scale k-distribution model for gas mixtures in hypersonic non-equilibrium flows," *Journal of Quantitative Spectroscopy and Radiative Transfer*, vol. 112, no. 7, p. 1213, 2010.

[15] H. Hu and Q. Wang, "Improved spectral absorption coefficient grouping strategy of wide band k-distribution model used for calculation of infrared remote sensing signal of hot exhaust systems," *Journal of Quantitative Spectroscopy and Radiative Transfer*, vol. 213, p. 17, 2018.

[16] V. Kez, F. Liu, J. L. Consalvi, J. Ströhle, and B. Epple, "A comprehensive evaluation of different radiation models in a gas turbine combustor under conditions of oxy-fuel combustion with dry recycle," *Journal of Quantitative Spectroscopy and Radiative Transfer*, vol. 172, pp. 121–133, 2016.

[17] L. S. Rothman, I. E. Gordon, R. J. Barber et al., "HITEMP, the high-temperature molecular spectroscopic database," *Journal of Quantitative Spectroscopy and Radiative Transfer*, vol. 111, no. 15, pp. 2139–2150, 2010.

[18] I. E. Gordon, L. S. Rothman, R. J. Hargreaves et al., "The HITRAN2020 molecular spectroscopic database," *Journal of Quantitative Spectroscopy and Radiative Transfer*, vol. 277, no. 11, Article ID 107949, 2021.

[19] Q. Niu, X. Duan, X. Meng, Z. He, and S. Dong, "Radiative heating analysis of a Mars entry capsule based on narrow-band K-distribution method," *Infrared Physics & Technology*, vol. 102, Article ID 103033, 2019.

[20] C. Caliot, Y. Le Maoult, M. El Hafi, and G. Flamant, "Remote sensing of high temperature H2O–CO2–CO mixture with a correlated k-distribution fictitious gas method and the single-

mixture gas assumption," *Journal of Quantitative Spectroscopy and Radiative Transfer*, vol. 102, no. 2, pp. 304–315, 2006.

[21] J. Taine and A. Soufiani, "Gas IR radiative properties: from spectroscopic data to approximate models," *Advances in Heat Transfer*, vol. 33, p. 295, 1999.

[22] Q. Niu, Z. Yuan, B. Chen, and S. Dong, "Infrared radiation characteristics of a hypersonic vehicle under time-varying angles of attack," *Chinese Journal of Aeronautics*, vol. 32, no. 4, pp. 861–874, 2019.

[23] F. Liu, G. J. Smallwood, and Ö. L. Gülder, "Application of the statistical narrow-band correlated-k method to low-resolution spectral intensity and radiative heat transfer calculations — effects of the quadrature scheme," *International Journal of Heat and Mass Transfer*, vol. 43, no. 17, pp. 3119–3135, 2000.

[24] J. R. Howell, M. P. Menguc, and R. Siegel, *Thermal Radiation Heat Transfer*, Taylor and Francis, Abingdon-on-Thames, UK, 2015.

[25] H. J. Nam and O. J. Kwon, "Infrared radiation modeling of NO, OH, CO, H 2 O, and CO 2 for emissivity/radiance prediction at high temperature," *Infrared Physics & Technology*, vol. 67, pp. 283–291, 2014.